Helical Klinotaxis: Simple Perception and Action Allows for Robust Stimulus Orientation

Adam C. Lammert

Vassar College
April 12, 2004

Senior thesis submitted in partial fulfillment of the requirements for the major in Cognitive Science

First reader: Dr. John Long
Second reader: Dr. Thomas Ellman

Contents

List of Figures

Abstract

Some animals that swim at low and intermediate Reynolds numbers (Re < 100) follow helical trajectories. These animals must also move towards and away from stimuli, a behavior that is essential for most animals. Hence, movement with respect to gradients involves effective alteration of the helical trajectory with respect to some sensory information about the gradient. An exemplar of such behavior in nature is that of swimming sea squirt larvae (Phylum Chordata, Subphylum Urochordata). Indeed, sea squirt larvae serve as an interestingly simple case, due to their limited sensorimotor capabilities. They have only a single directional sensor and a single degree of freedom in motor output. In contrast, most biological and robotic systems have at least two sensory inputs, which they compare to determine motor output. Previous work on how sea squirt larvae integrate sensory information with motor output, has suggested that the entire system, from perception to action, is simple. It is, perhaps, as simple as linear proportionality between input and output. Such work has involved the construction of models, in the form of robots and computer simulations. Expanding on previous work, this paper pursues the implementation of three additional models relating to this simple perception-action system. These models include (1) a surface-swimming robot that improves upon previous robotic testing by eliminating specific factors that have interfered with previous results, (2) a physics-based computer simulation of an aquatic agent that expands on previous theoretical work by offering an explanatory, rather than descriptive model and (3) a programmed terrestrial robot that demonstrates this systems position within the greater framework of robotics and specifically its connection to the influential work of Valentino Braitenberg.

1 Acknowledgements

John Long had the original inspiration for this work, as well as the moral and intellectual support to see me through it. Thomas Ellman and Cristian Castillo-Opazo and Mathieu Kemp formed the mathematical and implementational foundation for the numerical simulation. I also wish to thank John Vanderlee, Carl Bertsche and Lou Voerman for their perpetual assistance in designing and building the robot. Charles Pell and Catharina Berglund played a critical role in designing and building the robot and testing environment. Material support was provided by Vassar Colleges Department of Biology.

2 Introduction

The centerpiece of this work is a unique gradient orientation scheme, known as cycloptic helical klinotaxis (cHK). Cycloptic helical klinotaxis is a biological principle that has been observed in nature. Some organisms use it to perform gradient orientation in 3D. However, is not limited to 3D systems, and has been shown to work in both 2D and 3D (Long et al., in review). It is used by the larvae of sea squirts (Phylum Chordata, Subphylum Urochordata) to orient towards and away from light at low and intermediate Reynolds numbers (Re < 100). Also, cHK has been implemented and tested as a simple, robust form of navigation in autonomous underwater vehicles (AUVs) (Kemp et al., 2001; Kemp, 2001). One of the very interesting things about cHK is its sensorimotor simplicity. In the case of biology and AUVs, the agent performing cHK has only one sensory input and one kinematic degree of freedom, yet it can still effectively navigate with respect to a gradient.

The robot discussed here is different than sea squirt larvae in that it is restricted to 2D motion, however it shares the restrictions of a single sensory input and a single degree of freedom in motor output. Long et al. also used a robot that moved in 2D to investigate many of the same questions that are addressed herein. First, is a single sensory input sufficient for gradient-oriented navigation in 2D? Secondly, is a single kinematic degree of freedom sufficient for control of navigation in 2D? These issues, as might be expected, are functionally linked. The processes they involve are necessarily embodied in a common agent as part of a perception and action system (Chiel and Beer, 1997).

The reason for working with the same issues that (Long et al., 2003) did is that their experiments could stand to be improved upon. Certain experimental factors seem to interfere with interpreting the results, and a discussion of cHK could benefit from further experimentation. Specifically, interference from a small testing environment and the robots poor swimming ability may have substantially affected the trajectory of the robot. Thus, the first goal of this work is to further explore the adaptation and implementation of a biological principle (cHK) in an aquatic robot by making improvements on previous work.

As part of the effort to expand on previous cHK research, a computer simulation was also created. The purpose of this simulation is to model the forces acting on an idealized agent, an agent which is similar to the robot swimmer. The prediction was that a similar behavior would be observed in both the simulation and the actual robot. The reasons for making this simulation were threefold. First, it is an independent proof of the effectiveness of 2D cHK. Second, it illustrates the generality of this form of navigation. Third, it is possible that a simulation could be utilized to more easily test certain aspects of cHK navigation, such as how it holds up under different scaling conditions and extreme circumstances.

To further expand on the investigation of 2D cHK, one more set of experiments was performed. In these experiments, a digitally-controlled terrestrial wheeled robot was utilized to implement a variation on cHK, which is conceptually linked to the work on vehicle navigation by (Braitenberg, 1984). The

robot, with one sensory input, two driving wheels and a simple wiring connection between input and output, constitutes a vehicle of interest within the complex framework of synthetic psychology that Braitenberg lays out in his book Vehicles.

2.1 Background

Moving in a helix is comparable to locomoting by spiraling along on the threads of a screw. Despite how odd it might seem to animals with mostly linear motion (like ourselves), helical motion occurs commonly in microorganisms, spores of plants and fungi, larvae of some many invertebrates (Young, 1995), and less commonly in the larvae of some chordates (Long et al., 2003). Moreover, helical motion is the default for agents that travel at low Reynolds numbers. This is because most methods of propulsion involve asymmetrical deformations of the body, which cause both translation and rotation (Purcell, 1977). Any motion that involves both translation and rotation is helical.

The trajectory of helical motion can be controlled by modulating only the rotation of the agent. Rotation is the only degree of freedom necessary to create the complex trajectories inherent in helical motion. No adjustment of translation is necessary for altering the axis of the helix (Crenshaw, 1993a,b). Moreover, a proper coupling of gradient information with the rotation of the agent allows for gradient orientation, which is desirable for many agents (Crenshaw, 1996). Most agents find it necessary to navigate with respect to sensory gradients at some point. Such behaviors allow animals to locate mates, avoid predators and find food. This gradient-oriented behavior using helical trajectories is otherwise known as helical klinotaxis (HK), where klinotaxis refers to orientation strictly by use of vector information (Fraenkel and Gunn, 1940). Cases where only one sensor is needed to successfully allow for HK will be referred to as cycloptic HK, or cHK, through the course of this paper.

The sensory information about a gradient must be crucially linked to the agents rotation to allow HK. However, such a coupling need not be very complicated. Nor is it necessary for the sensory information, or the method of altering rotation, to be complex. Crenshaw (1996) clearly explains that HK can occur if the sensory information is no more than intensity readings. Also, the components of rotation can be altered as simple functions of stimulus intensity. McHenry and Strother (2003) found that the larvae of ascidian sea squirts performed HK in precisely this way. In agreement with Crenshaw (1996), they found that the components of rotation were simple functions of sensory information (Figure 1). In this case, the sensory information is gathered by a single, directional photoreceptor (ocellus), measuring light intensity. The components of rotation, yaw, pitch and roll, are controlled by the asymmetry of a steadily beating tail. The function which determines how the tail asymmetry (and, in turn, the rotation) is affected by the stimulus intensity is a simple direct proportionality. That is, the angle of the beating tail becomes asymmetric in direct proportion to the sensed intensity of the light.

The first work that used HK for robotic implementation was that by Nek-

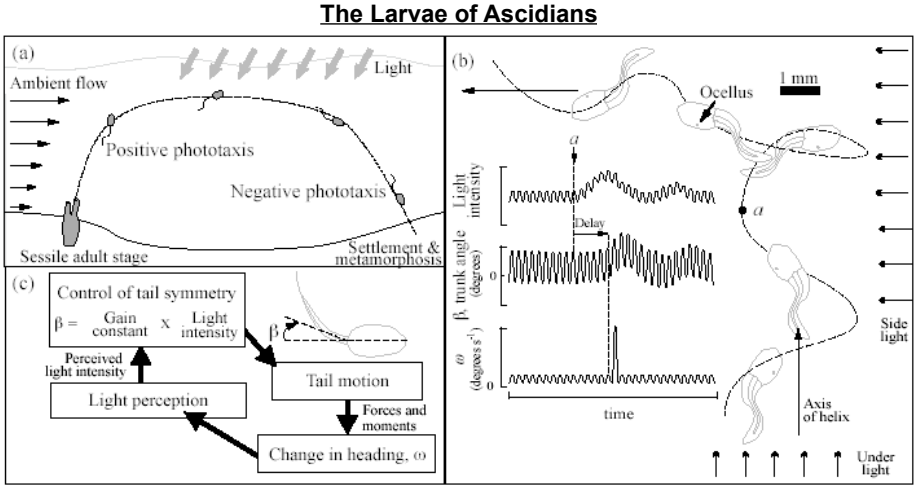

Figure 1: The larvae of ascidians perform phototaxis for the purpose of dispersal of offspring. Figures used here were taken directly from (Long et al., 2003). (a) Adults ascidians are sessile organisms that remain attached to the ocean floor substrate. The adults release their offspring in the form of swimming larvae. These larvae initially perform positive phototaxis and, consequently, move up toward the surface. Ocean currents carry the larvae away from their sessile parents as they swim. Eventually, the phototaxis turns negative and the larvae begin to move down towards the substrate. Once the substrate has been reached, the larvae attach themselves to it and mature into their adult form. (b) Changes in the direction of the light source cause a slow oscillation in light intensity to occur at the ocellus. To correct for this, the larvae must alter their propulsion to change direction. Observations of ascidian larvae by (McHenry and Strother, 2003) indicate that, to do that correction, their tail beats become more or less asymmetric in response to the intensity of light. (c) McHenry and Strother (2003) hypothesized that the asymmetry of tail beats, β, varies in proportion to light intensity.

ton Research (Durham, NC, USA). Their Microhunter^{TM} AUV performs HK navigation by using a single propeller. Modulating that propeller allows the platform to alter both rotation and translation, and thus change the axis of its helical path (Kemp et al., 2001). The fact that modulation of the propeller alters translation, in addition to rotation, is one level of difference between this technology and the kinematic theory of HK (Crenshaw, 1993a,b, 1996). Moreover, Microhunter^{TM} fails to operate in the way that the kinematic theory predicts. Indeed, the control scheme used for altering the helical trajectories of the robot is dynamical in nature (Kemp, 2001). This work by Nekton was, nonetheless, the first time that HK had been used to control artificial agents, and this technology is patented and assigned to Nekton Technologies, Inc. (US patent #6,378,801; 30 April 2002; inventors Pell, Crenshaw, Janet, Kemp).

HK is a very simple, yet effective, method of navigation. It stands as a completely reactive control architecture, with no environmental modeling involved. As such, it deals very well with functioning in complex, dynamic environments (Russell and Norvig, 2003). Moreover, it is simple even compared to other reactive architectures, in both implementation and function. It offers the ability to orient to gradients with only one sensory input (in cHK). It is commonly assumed that, to properly orient, two sensors are required to make a spatial comparison between points in the gradient (Braitenberg, 1984; Arkin, 1998). Moreover, when one sensor is used, it is assumed that temporal comparisons need to be made (Murphy, 2000). This is essentially the same as making a spatial comparison, as long as the agents sensor is moving through space. Such spatial comparision occurs in E. coli, Paramecium and the nematode, C. elegans (review in Morse et al., 1998). However, cHK is able to operate under what, by comparison, might seem like a severe lack of sensory information. Only one sensory input in needed, with no added computational baggage occurring behind the scenes.

No matter where the comparison-style systems hide it, an increased level of complexity is required for them to work. That is, they have a greater amount of complexity than cHK. If the implementation of comparison-style gradient detection utilizes spatial comparisons, an increase in the number of sensors is necessary. Additionally, either type of comparison, whether spatial or temporal, requires an added level of complexity in perception (*sensu* Kelley, 1986) by the very design of the system. A comparison must be made, and that requires an extra step on the way from sensation to action.

HK also offers the ability to navigate in complex spatial environments with required control over only one variable. In larger animals, such as fish and whales, HK is apparently absent. These animals stabilize their roll at the sacrifice of necessitating more actuation (i.e. fins and flippers) to exercise control over more variables (Long et al., 2003). This increased control allows larger animals to perform turns in 2D only. However, navigation with respect to gradients in 2D also operates by way of controlling rotation, and therefore is a special case of HK (Long et al., 2003). This implies that there is a definite link between HK in 3D and 2D. Indeed, it has been shown, empirically and kinematically, that

2D HK is possible with the control scheme that allows sea squirt larvae to orient to light in 3D (Long et al., in review).

2.2 Aquatic Robot

In an investigation of cHK, Long et al. (2003) built and tested a robot that implemented 2D cHK. The control of this surface-swimming robot was based on the ideas proposed by McHenry and Strother (2003) about how sea squirt larvae perform cHK. The larvae orient to light gradients by altering the asymmetry of their tail beats in direct proportion to light intensity. The surface-swimming robot mimicked this behavior with the use of an analog electronic circuit. This was the first time that a 3D HK control scheme had been utilized to control a robot restricted to 2D. Despite the reduction in dimensions, the robot effectively oriented to light by performing cHK.

The work of Long et al. (2003) not only provides support for the cHK control mechanisms proposed by McHenry and Strother (2003), but it also highlights a very real connection between HK in 2D and 3D. The fact that the exact same control mechanisms work in both spatial environments, then HK must be a rather robust and generalized form of locomotion. Indeed, it was even found that if a single sensor was used on a wheeled terrestrial robot and only rotation was modulated with respect to the sensor reading, 2D cHK could be carried out on land as well. The higher frictional forces and different style of actuation did not interfere with the effectiveness of 2D cHK. Moreover, it might be possible for some agents to switch back and forth between 2D and 3D versions of the same locomotion scheme, since both are cases of HK (Long et al., 2003).

Long et al. (2003) were trying to make a point for an engineering audience about the generality of HK, but just as importantly about the simplicity and ease of implementation associated with HK. As a result, their experimental robots left some things to be desired. Primarily, the analog surface-swimming robot that they used left lots of room for improvement in terms of effectiveness of swimming ability. Specifically, effectiveness was lacking in the amount of thrust production and the direction of thrust production (i.e. it was not in line with the tail angle). The robot also lacked precision in keeping tail asymmetry proportional to light intensity. Moreover, the experiments involved problems with the testing area (namely the small size of the water tank) that caused some problem in interpreting the results. Interactions between the robot and the walls strongly affected the motion of the robot in some cases, raising questions about the actual effectiveness of the robots phototactic abilities.

The first set of experiments described in this paper aimed to improve upon those performed by Long et al. (2003). The testing environment was increased in size and depth. These improvements will eliminate possible wall interferences that were a detriment to the experiments of Long et al. (2003). Also, improvements were made to the robot itself. The hope was to give the robot a better propulsive system and a tighter control over its rotational velocity. However, it should be noted that the robotic improvements proposed here were intentionally left out of the Long et al. (2003) robot, because of their focus on HKs ease of

implementation. With that being said, it is my contention that a robot which can more effectively swim and can more accurately execute its control scheme, even despite an increase in design complexity, will allow better data to be taken. As a result, the empirical support for 2D cHKs effectiveness will be strengthened. It is believed that this goal is not at odds with the work of Long et al. (2003), but complementary to it.

2.3 Simulated Agent

As robots are becoming an increasingly popular tool for modeling behavior (Webb, 2002), it is increasingly a point of debate as to whether robots or computer simulations have more advantages in modeling. Robots offer a safeguard against unrealistic assumptions, because they are situated in, and interacting with, a real-world complex environment (Brooks, 2002). This fact makes it easy to observe, more accurately, the effect of factors like environmental signals, noise and how actions in the environment might have consequences (Webb, 2002). However, computer simulations have much to offer, as well. Simulations allow, in many cases, easier manipulations of behavioral variables and more accurate detail in implementation (Webb, 2002). Since both types of models seem to have their own advantages, it seems that the best solution is to have both and allow them to complement each other. Indeed, this is becoming increasingly common (Webb, 2002). The case of 2D cHK is no exception to this.

In the interest of further exploring the generality of 2D cHK, Lammert and Long (2003) created a computer-based simulation of the aforementioned swimming robot (Long et al., 2003). This simulation attempted to recreate only the kinematics of the robotic system. Strong assumptions were made that included lack of frictional losses, no sensorimotor delay and constant translational velocity (Lammert and Long, 2003). Hence, the simulation was a level of abstraction apart from the robotic system. However, its main purpose was to offer another test of 2D HKs generality. The results of the simulation building showed phototactic behavior, as qualitatively described by Lammert and Long (2003). Thus, the simulation showed, once again, support for the generality and the effectiveness of HK.

A far more refined and precise exploration of 2D cHK kinematics came with the later work of (Long et al., in review). There, an analytic solution to the kinematics of cHK was pursued and found. Phototactic behavior in 2D cHK is the product of the vehicle constantly adjusting its heading, such that the rotational component of its movement can be nulled (Long et al., in review). Moreover, because this is the case, phototactic behavior only holds for standard sensor placements (i.e. a forward-facing sensor). Interestingly, different sensor locations dont cause the system to break down, but merely change the nature of the behavior. Sensor placement near 90 degrees results in a wandering behavior, where the agent never truly holds steadily at the source. Furthermore, a sensor location near 180 degrees shows a negatively phototactic behavior (i.e. repellant) (Long et al., in review). This dependence on sensor placement is, perhaps, not surprising. Indeed, 3D HK systems also show a dependency of sensor location to

properly perform HK. However, in 3D HK, the sensor location matters because changes in rotation must be phased correctly with respect to the source of the gradient (Long et al., in review).

The second set of experiments in this paper aimed to create a new simulation, which builds off of the work of (Long et al., in review). By taking into account even very simple dynamics, it is hoped that this simulation will serve as a more explanatory model, in contrast to the descriptive nature of the kinematic simulation. The kinematic simulation is a highly idealized model which does an excellent job of showing how phototactic behavior can result from a description of the agents motion. However, it is hoped that a dynamics-based simulation will provide more of an explanation of how the mechanisms of this perception and action system lead to the motion of the robot, which consequently results in phototaxis.

2.4 Vehicle 1.5

The influential work of (Braitenberg, 1984) gives insight into how simple internal structures and basic control schemes can lead to surprisingly complex behaviors. By analyzing behavior from the bottom up, in what he calls synthetic psychology, a whole gamut of (sometimes unpredictably) complex behaviors arise from simple, deterministic mechanisms (Pfeifer and Scheier, 1999). In many ways, this is the sort of observation that can be made concerning cHK, as well. One sensor and one control variable are sufficient for its operation. Moreover, the control scheme for integrating sensors and motors can be strikingly simple. It could be said that HK and the behaviors displayed by Braitenbergs vehicles are examples of behavioral primitives (sensu (Long et al., in review). That is, behaviors which are irreducibly simple in execution and implementation. However, where does an HK system fit into Braitenbergs discussion, if anywhere? To fully appreciate the answer to this, one must first understand, or review, some of Braitenbergs earliest points of discourse.

Appropriately, Braitenbergs discussion begins with the simplest configuration, and proceeds from there to the more intricate implementations. His first vehicle, or Vehicle 1 as he calls it, is merely a one sensor and one motor with a connection between the two. The sensor is placed at the farthest point forward on the vehicle and picks up information about the quality of a given stimulus (e.g. temperature). The motor is placed at the farthest point to the rear of the vehicle and is mounted as to push the vehicle forward. The connection is a very simple one. The stronger the stimulus signal is at the sensor, the faster the motor turns. Hence, the motors speed is proportional to the stimulus reading (Braitenberg, 1984).

Vehicle 1 does display a behavior, albeit a very simple one. Functionally, the vehicle will speed up in areas where there is more of the stimulus, and will slow down where there is little. As a behavior, this can be described as an affinity for less of the stimulus, or perhaps an aversion to more. Certainly, the motor for Vehicle 1 only pushes in one direction. However, in a real-world environment with friction and other obstacles to motion, the vehicle would move

on a, more or less, unpredictable path. If the robot is small enough, the vehicles motion might even seem randomly Brownian. However, the speed of the motor would still ensure that the vehicle would speed up and slow down according to the stimulus gradient. Thus, it would probabilistically spend more time in the low-stimulus areas, but would be very bad at finding those spots (Braitenberg, 1984).

The type of motion that vehicle 1 performs is often referred to as a kinesis. Also, it has been described as a biased random walk (Fraenkel and Gunn, 1940). Essentially, the motion is undirected, but has a bias with respect to the stimulus. This type of behavior is often seen in microorganisms, notably in the chemo-orientation of bacteria (Crenshaw, 1996). Braitenberg called it restlessness, as a way of tying into (synthetic) psychology (Braitenberg, 1984). Certainly, it is a fine common-sense description.

A simple increase in the complexity of Vehicle 1 leads us to Vehicle 2a, and out of the realm of kinesis. Technically, the motion that shows true directedness to it is often called taxis (Fraenkel and Gunn, 1940). Tactic behavior shows control of orientation (Crenshaw, 1996), and does not need to rely on elements of motion randomization to find its way. So, what sort of system is needed for Vehicle 2a to execute this? As Braitenberg describes it, Vehicle 2a results from sticking together two Vehicle 1s. If two copies of the first vehicle are stuck together, side by side, and allowed to move, tactic behavior is the result (Braitenberg, 1984).

The system in Vehicle 2a works thusly: Whichever sensor detects more of the stimulus will cause the corresponding motor to work harder. Consequently, the vehicle will turn away from the source. After turning, the vehicle will then slow down due to the lower stimulus intensity. Thus, the vehicle is repulsed by the stimulus. Braitenberg referred to this behavior as fear. It is, more technically, called negative taxis. Positive taxis, interestingly, can be implemented by simply crossing the connections, so that the right sensor is connected to the left motor, and vice versa. This variant vehicle, called Vehicle 2b, will turn towards the gradient source and speed up as it gets closer. This behavior was called aggression (Braitenberg, 1984).

The description of Vehicle 3 also sees the introduction of a different type of sensorimotor connection, a negative, inhibitory connection. This type of connection gives a decreasing signal as more of the stimulus is detected. By substituting this type in for its positive counterpart in Vehicles 2a and 2b, some interestingly different behaviors arise. Vehicle 3a, with uncrossed inhibitory connections, will seek the source of the gradient and slow down as it approaches. This type of positive taxis was what Braitenberg called love. Vehicle 3b, with its crossed inhibitory connections, will speed up away from the source, only to return for a slow pass-by. This behavior was called by Braitenberg exploration. In any case, the first three vehicles use a palette of only two sensors, two motors, and two types of connections, yet the resulting behaviors are different and of increasing complexity (Braitenberg, 1984).

So where, if anywhere, does cHK fit into this discussion? It seems like Braitenberg took the smallest steps possible in increasing the complexity of his

vehicles as he proceeded from Vehicle 1 up through Vehicle 3. A vehicle that performs cHK only needs one sensor, much like Vehicle 1 has. However, cHK is controlled on the motor end by modulating rotation. Such modulation is not possible with the motor system that Vehicle 1 has. Its single motor is only able to adjust translation. If the wheel were restricted to turn at a constant rate, and was controlled instead by swiveling, rotation could be modulated. In fact, a system like this would be very similar to that of the sea squirt larvae and the surface-swimming robot. However, that type of configuration doesnt seem to fit into the overall course of Braitenbergs discussion neatly.

Another way to enable the vehicle with rotational control is to implement the motor configuration used in Vehicle 2a. That vehicle has two wheels on either side of the robot, which does provide rotational control. Moreover, it is used early on by Braitenberg, so it flows nicely with his discourse. Thus, our cHK vehicle would need two motors and one sensor. Perhaps this new vehicle could fit neatly into Braitenbergs discussion between Vehicle 1 and Vehicle 2, then. It is Vehicle 1.5, if you will.

However, Vehicle 1.5 only belongs there if it can be implemented using the simple types of connections that Braitenberg used. Indeed, it may be possible to do just that (Figure 2). First, the single sensor will need to be connected to each motor to allow control of rotation. However, making both connections positive would be pointless, since the result would be essentially the same as Vehicle 1. If we are allowed to reach ahead in the discussion and use the inhibitory-style connection from Vehicle 3 for both of the motors of Vehicle 1.5, the result would be the same as Vehicle 1 again, except in reverse. That is no help either. However, if we connect one motor using the excitatory connection and the other with an inhibitory one, we should get what we want. The resulting vehicle would use information from one directional sensor to adjust the amount of rotation the vehicle performs. However, the rotation would arise very differently in Vehicle 1.5, as compared to the aquatic robot. Instead of rotation coming from the orientation of the thrust vector, it would instead come from differences in the thrust of the two wheels. Still, such a system would be performing cHK so long as it could adjust rotation in proportion to light intensity. Intuitively, that is exactly what should happen with this vehicle. However, since cHK is sometimes difficult to visualize, empirical findings would certainly strengthen the case for Vehicle 1.5, and its ability to perform 2D cHK. Such empirical findings are just what this paper aims at uncovering, in the third set of experiments.

3 Methods

3.1 The Aquatic Robot

The aquatic robot used for the experiments herein (Figure 3) should bear significant resemblance to the robot used by (Long et al., 2003). This is due to the aforementioned reason that these experiments are an attempt to repeat, and improve, upon the original ones.

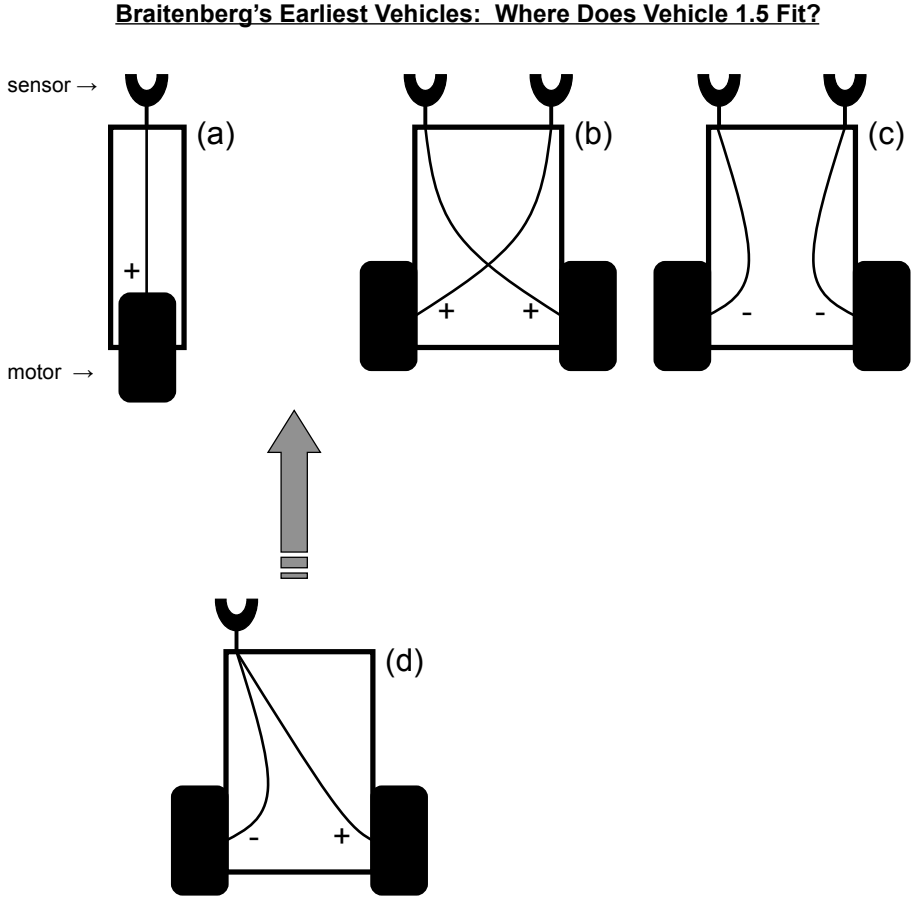

Figure 2: Braitenberg's vehicles 1 through 3 and vehicle 1.5. (a) Vehicle 1 has only one sensor and one motor, with a single, excitatory connection between the two. It is capable of avoiding areas of high stimulus intensity through kinetic means. (b) Vehicle 2b has two sensors, two motors and two excitatory, crossed connections. It is able to seek out light sources and accelerate towards them. It does this in a truly tactic way. (c) Vehicle 3a has two sensors, two motors, and two straight, inhibitory connections. This vehicle can perform tactic behavior to seek out light sources and stay near them. (d) Vehicle 1.5 has two motors and two connections, but only a single sensor. It is capable of seeking out light sources by performing 2-dimensional cycloptic helical klinotaxis (2D cHK).

The hull of the aquatic robot was made from a flat-bottomed, right-circular, tapering plastic container (Tantarelli 20C). The shape approximated the bulbous shape of the sea squirt larvaes anterior section. However, the chosen container was round, rather than elliptical, in order to simplify the dynamic, computer simulation of this robot. The hull contained electronics, batteries and a plumb-bob for ballast (50 g). The propulsive unit was adhered to the aft of the robot with the use of epoxy. When completely constructed, the robot had a displacement of 718 $\pm$ 54 cm^3 ($\pm$ std. dev). The diameter of the container at the waterline was 16.4 cm, with a draft of 2.6 cm and freeboard measuring 4.0 cm. Using the hull length at the waterline as the characteristic length, the experiment-time Reynolds number of the robot ranged from 5217 to 14888. This is more than 3 orders of magnitude above that of the sea squirt larvae. Thus, our robot was experiencing a system more highly dominated by inertia. By comparison, the system in which sea squirt larvae move is dominated by skin friction and form force (McHenry and Strother, 2003).

The movement of the aquatic robot was controlled with the use of two motors, one for propulsion and one for asymmetry. The propulsive motor was a standard rotary motor (RadioShack; 1.5–3.0 VDC; 8700 RPM $\pm$ 12% at no load), used to drive the laterally-oscillating tail. This laterally oscillating tail was intended to imitate a similar tail in sea squirt larvae (McHenry and Strother, 2003). To create the lateral motion, the propulsive motor was attached to a reduction gear box with a sliding crank. This sliding crank operated at a constant frequency of .56 $\pm$ .01 Hz ($\pm$ 1 std. dev.). The amplitude was also constant at 5.4 $\pm$ .21 cm ($\pm$ 1 std. dev.). Since there is an inherent asymmetry in the operation of sliding cranks (due to changing length of the moment arm) the lateral tail motion of the robot was temporally asymmetric. That is, a full excursion of the tail to one side was slightly quicker than to the other side. The terminal tail blade was fashioned with duct tape in the shape of a rectangle 4.6 cm in length and 3.2 cm in height. The tail blade was 0.1 cm thick, or about 4 plies of duct tape.

The asymmetry of the tail position was controlled by a standard servomotor (Maxx Products; MPI MX-400) on which the entire propulsive unit (motors, gears, crank and tail) was mounted. With the propulsive unit attached to the head of the servo, the base unit was then turned head-side-down and mounted directly in the rear of the hull with a waterproof epoxy. The servo was restricted to a 90 degree range of motion. The use of a servo is one major difference between this robot and the robot used by (Long et al., 2003). It was my hope that the precision of a servo, as well as its ability to hold position would be a substantial improvement on accuracy of locomotion. The motorized potentiometer that (Long et al., 2003) used had a lower level of angular precision and an inability to recognize or hold positions like a servo.

The only sensory input was provided by a cadmium sulfide photoresistor (20kΩ). This type of sensor varies its resistance with respect to light intensity. Only one side of the sensor is responsive to light, thus adding an element of directionality to the sensor. Moreover, this directionality was enhanced by mounting the sensor on a small, flat piece of cardboard (5cm $\times$ 3cm), with

The Aquatic Robot

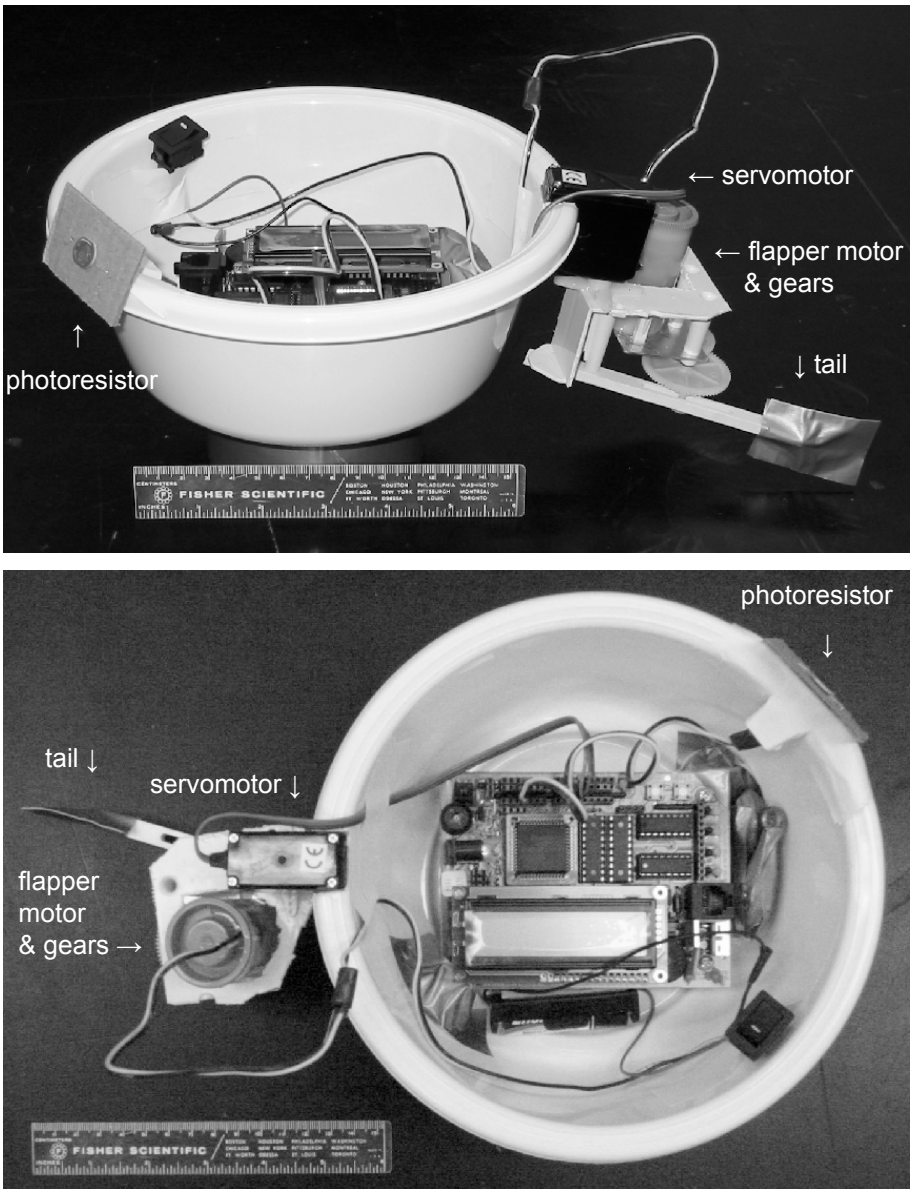

Figure 3: Photographs of the aquatic robot. The first picture is a view from the side of the robot, and second picture featured was taken from above the robot. The photoresistor, servomotor, flapper motor, gear train and tail can all be seen and are labelled.

the sensitive side facing away from the cardboard. This was to further limit the amount of light hitting the sensor from the opposite side. The sensor was mounted 45 degrees left of direct center on the front of the robot (i.e. 135 degrees away from where the servo was mounted, around the circular body). This type of sensor and its orientation on the body were intended to imitate the actual ocellus of a sea squirt larva.

Integration of the sensor and servomotor was provided by connecting each to the ports of a microcontroller (the MIT Media Laboratory's HandyBoard). Programming was done in the Interactive C programming language (Figure 4). The simple program perpetually checked the sensor reading, and then rescaled that number to make it an angle instruction for the servo. This allowed the angle of the servo and the entire tail unit to change its angle in response to a change in stimulus intensity at the sensor. The angle of the tail, then, was always kept in linear proportion to the sensor reading.

However, it should be noted that the sensor reading is rather different than the absolute light intensity. This is a major problem if the goal is to have the tail angle be proportional to light intensity. The reason for the discrepancy lay in the nature of cadmium sulfide photoresistors. These types of sensors tend to change their signal in an inversely linear fashion with distance from a light source. Light intensity, by contrast, tapers as the inverse square of distance. However, the further away from the light source one gets, the more linear the light intensity function becomes. Fortunately, the point at which both functions begin to look reasonably linear is not very far from the source. Hence, the sensor reading at that point was used as a bright-end (low-reading) limit. Sensor readings that are brighter would be rather unrepresentative of the actual light intensities, which is undesirable. In the trials discussed here, the brighter limit on the sensor readings was 5, occurring approximately .5 m from the light source. Although the values are small, this limit does represent the brighter side of sensor readings. There was also a limit placed on the other, dimmer end of sensor readings. Essentially, this was to make the robot only sensitive to light intensities found within the bounds of the testing area. In this case, the maximum relevant sensor reading was 100, occurring at approximately 1.3 m from the light source. Thus, the sensor values could range from 5 to 99, and within this range the functions for sensor values and light intensity values were of roughly the same shape. This attempt to make the values more accurate to the light intensities was not addressed in the work of (Long et al., 2003), and this constitutes an attempt to improve upon those experiments.

The liquid crystal screen of the microcontroller was used to display the sensor readings in real time during the experiments. This was for the purposes of additional data collection.

3.2 The Simulated Agent

The dynamical model of the robot was developed with respect to three crucial variables. These variables are x and y, which mark the position of the robot on a standard Cartesian coordinate system, and θ which is the angle of orientation

The Aquatic Robot Program: 2D HK

```
#use "servo.icb"
//----------------------definitions-----------------------------
#define BETA_MIN 0.0
#define BETA_MAX 120.0
#define SENSOR_MAX 45.0
#define SENSOR_MIN 5.0
#define SERVO_TIME 50L
#define SERVO_RANGE (MAX_SERVO_WAVETIME-MIN_SERVO_WAVETIME)
#define rexcursion 3.14159
#define dexcursion 180.0
#define REMOTE_BUTTON 80
//-----------------------declarations-----------------------------
float Beta;
int Sensor_int;
float Sensor_float;
float Seconds = seconds();
int Whole_Seconds = (int)Seconds;
int Num_Seconds = 10;
int Print_Period = Whole_Seconds%Num_Seconds;
int Print_Track = Print_Period;
//------------------------program---------------------------------------
void main()
{
     msleep(500L);
     servo_on();
     while(1)
          {Seconds = seconds();
            Whole_Seconds = (int)Seconds;
            Print_Period = Whole_Seconds%Num_Seconds;
            Sensor_int = analog(3);
            Sensor_float = (float)Sensor_int;
            if(Sensor_float > SENSOR_MAX)
              Sensor_float = SENSOR_MAX;
            if(Sensor_float < SENSOR_MIN)
              Sensor_float = SENSOR_MIN;
            Sensor_int = (int)Sensor_float;
            Sensor_float = 50.0 - Sensor_float;
            Beta = ((BETA_MAX/SENSOR_MAX)*Sensor_float) +
                  ((dexcursion-BETA_MAX)/2.0) + 15.0;
            servo_deg(Beta);
            if((Print_Period)==0 && (Print_Period)!= Print_Track)
              {if(Sensor_int>9)
                  printf("%d", Sensor_int);
                else
                  printf("0%d",Sensor_int);}
        Print_Track = Print_Period;}}
```

Figure 4: The complete aquatic robot control program.

of the robot, where 0 occurs when the robot is pointing directly along the x-axis. The positional variables can be put into a vector called X, such that $X = (x, y)$. We incorporate this into Newtons law in order to determine the dynamics thusly:

$$\ddot{X} = \frac{F}{m}. \tag{1}$$

Now, the forces, F, acting on the robot are thrust and drag. For the sake of simplicity, the thrust is represented as a constant T. Drag is $D = 0.5\rho s c_d \dot{X}$, a standard equation (Halliday et al., 2001), where ρ is the density of the robot, s is the wetted surface area of the robot and c_d is the coefficient of drag. Thus, our equation becomes,

$$\ddot{X} = \frac{Tcos(\beta) - 0.5\rho s c_d \dot{X}}{m}, \tag{2}$$

where β is the angle between the tail and the body, with 0 occuring as the tail comes into alignment along the long axis of the robots body.

Assuming that acceleration of the robot is irrelevant to this method of phototaxis, we can then model the robot as it moves at a steady state with thrust and drag balanced. Thus, we set $\ddot{X}$ to 0 and solve for $\dot{X}$ to get,

$$\dot{X} = \sqrt{\frac{2Tcos(\beta)}{\rho s c_d}}. \tag{3}$$

It is understood, however, that the assumption of no accelerations may not always hold true of the actual system, and as such may introduce some small amount of error into this model. There may, indeed, be some acceleration of the aquatic robot, for instance, at the very start of a given trial and during tight turns. It is firmly believed, though, that accelerations are unimportant to the cHK behavior and, thus, any error introduced by this assumption is minor.

Now this equation is broken into components to determine $\dot{x}$ and $\dot{y}$:

$$\dot{x} = cos(\theta)\sqrt{\frac{2Tcos(\beta)}{\rho s c_d}}, \tag{4}$$

and,

$$\dot{y} = sin(\theta)\sqrt{\frac{2Tcos(\beta)}{\rho s c_d}}. \tag{5}$$

The rate of rotation is determined by the angle β times a constant k, such that,

$$\dot{\theta} = k\beta. \tag{6}$$

The angle β is determined by a piece-wise function, dependent on the intensity of the stimulus. If the perceived intensity of the stimulus is above or

below a certain window (I_{min} to I_{max}), then β is at β_{max} or β_{min}, respectively. However, within the given window, β is linearly proportional to the intensity of the stimulus. This is just the way that the angle of asymmetry was determined in the aquatic robot.

The perceived stimulus intensity is a function of the inverse square of distance from the source and, also, the orientation of the sensor as follows:

$$I_p = \left(\frac{I}{(x^2 + y^2)^{-1}} \right) a, \tag{7}$$

where,

$$a = sin \left(\frac{\theta + \delta - \phi}{2} \right), \tag{8}$$

where δ is the angle between the orientation and the sensor, and ϕ is the polar angle of the robot around the source.

This system of equations was then formatted as a Mathematica^{TM} notebook (Figure 5), solved numerically and graphed by means of a parametric plot of x and y. This allowed a clear view of the motion of the simulated robot. Several different sets of initial conditions were solved and graphed for observation. These initial conditions showed the robot as beginning in at different locations around the gradient source, and in different initial orientations.

3.3 Vehicle 1.5

To implement Vehicle 1.5, the Rug Warrior Pro Mobile Robot Kit (A K Peters, Ltd.) was used. Although the digital microcontroller of the Rug Warrior is certainly overkill for a system as simple as this, it was a readily available terrestrial robotic system with several aspects that were an immediate advantage. Namely, this robot has a two-wheel differential drive and a cadmium sulfide photoresistor mounted in the exact position that was needed (45 degrees left of the immediate front). The directionality of the photoresistor was enhanced by adding a small flat (5cm $\times$ 2cm) panel behind the sensitive side of the sensor. This panel was similar to the one used for the aquatic robots sensor, and was also made from cardboard.

The sensorimotor connections of Vehicle 1.5 were implemented in a fashion similar to the aquatic robot. The Rug Warrior can be coded in Interactive C, much like the Handy Board (Figure 6). Thus, a simple program was written that used information from the photoresistor to adjust two variables. The rescaled photoresistor reading was added to one variable and subtracted from the other, thus making these two variables exact complements of each other. Moreover, these variables then corresponded to the excitatory and inhibitory connections of Vehicle 1.5. Subsequently, the variables were used to drive the left and right motors. The Rug Warriors liquid crystal screen was used to display the sensor reading in real time during the experiments. This was for the purpose of additional data collection.

The Vehicle 1.5 Program: 2D HK

```
int lightL;
int lightR;
float system_time = seconds();
int system_time_int = (int) system_time;
int interval = 2;
int flag = 1;

void main()
         {sleep(0.5);
             while(1)
                {system_time = seconds();
                  system_time_int = (int) system_time;
                  lightL = analog(1);

                    if(lightL>99)
                    lightL=99;

                  lightR=99-lightL;

                  motor(0,lightL);
                  motor(1,lightR);

                  if((system_time_int%interval)!=0)
                    flag=0;
                  if(((system_time_int%interval)==0) && (flag==0))
                    {flag = 1;
                      if(lightL<10)
                        printf("0%d",lightL);
                       else
                        printf("%d",lightL);}}}
```

Figure 5: The complete Vehicle 1.5 control program.

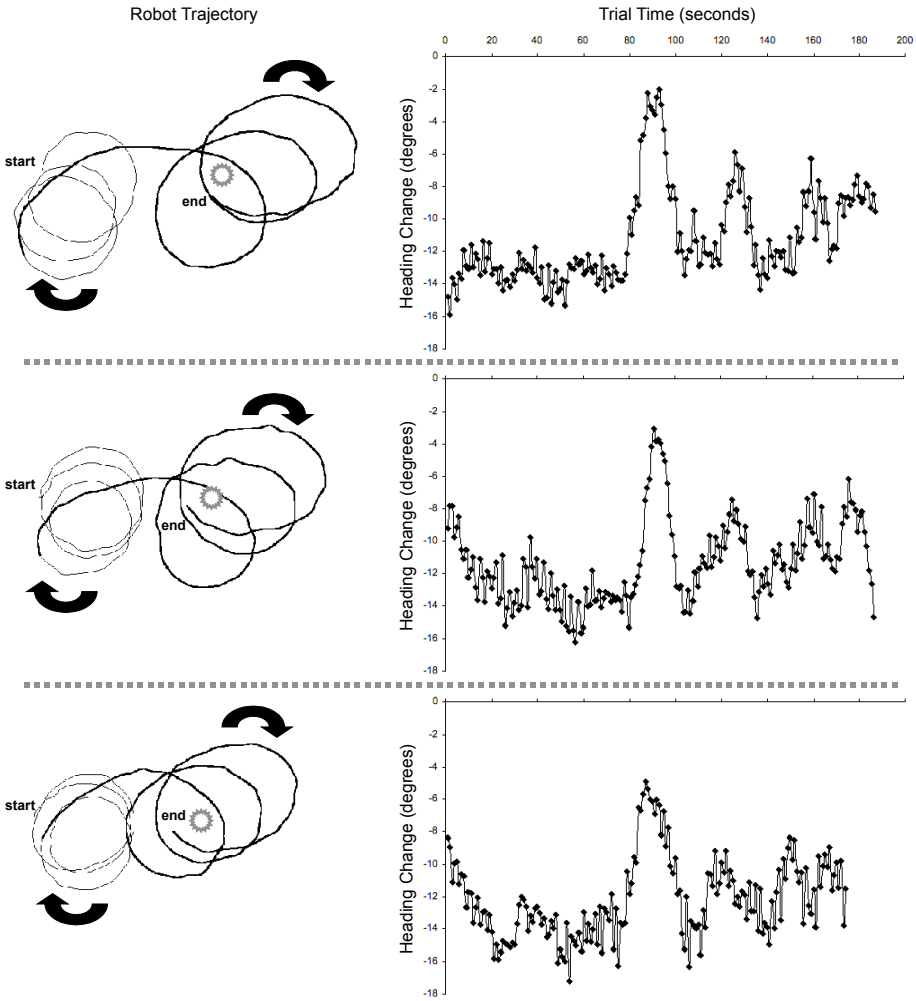

Figure 6: The aquatic robot was put through three trials, shown from top to bottom. Trajectory graphs are shown to the left, and to the right are the corresponding graphs showing heading change over the course of the trials. The starting and ending positions are labelled, as is the point of maximum light intensity (sun symbol). The direction of rotation is also indicated with arrows. The heading change graphs display the data after an 11-point central running average was performed

3.4 Experiments

The experiments with the aquatic robot were performed in a rectangular water-filled tank of the size 2.4 m by 2.5 m. The depth of the water was .12 m, and the water temperature was 15°C throughout the trial. The air temperature was 23°C. The tank was made by nailing four 2×10 pine boards into a rectangular formation, and then draping two large waterproof tarpaulins inside, one on top of the other, to act as liners. This tank was much larger than the one used by Long et al. (2003a), and the hope was that it would help eliminate any interaction between the robot and the walls of the tank. Such interactions were a negative aspect of the experiments described in (Long et al., 2003).

The light source used was a 40W incandescent light bulb that was hung, bare, .2 m over the waters surface in the center of the tank. A light gradient was created that was typical of this type of bulb. Light intensities were measured using a photometer held at 90 degrees perpendicular to the waters surface, facing the bulb, and 3 cm above the surface. The point of highest intensity was measured at .1 m away from the source, and was 937 lx ± 28.5 (± 1 st. dev). The intensities were measured out to 1.5 m from the source, where the lowest intensity was measured at 33 lx ± 0.0 (± 1 st. dev). The decrease in intensity with distance was roughly equal to the inverse square of distance, as should commonly be expected of any light gradient (regression is $y = 68.4x^{-1.33}$; $R2 = 0.97$).

The functioning robot was placed in the tank, facing half-way between directly at the light and directly away. Initially, the light was off and there was no light gradient. This initial period with no source was to act as a control, to which a comparision could be drawn. This comparison would be more illustrative of the robots behavior in the presence of a source. Without a source present, the robot tended to rotate clockwise. After the robot had rotated three times, the light was turned on. Once the light source was turned on, the robot also continued to rotate, but tended to rotate around the source. Thus, once the light was turned on and robot rotated another three times, the trial was ended. Three trials of this type were conducted.

Recordings of the trials were made using a digital camcorder mounted directly above the tank, pointing down. This camera captured the whole tank. The video was analyzed using motion-analysis software (VideoPoint). This software allowed a Cartesian coordinate system to be overlain on individual frames of the video, with the origin placed at the center of the tank and the x-axis extending negatively through the light source. Then, several points were tracked in each frame with respect to that coordinate system. Among the points tracked were the immediate front and back of the robot, which were used to calculate the heading of the robot. A heading of 0 degrees was understood to be the robot moving directly in line with the x-axis, in the positive direction. These points were also used to calculate the change in heading, and their midpoint was used to determine the position of the robots center of mass.

Sensor readings, as displayed on the robots LCD screen were copied down onto paper for later analysis. The sensor readings were calibrated to light inten-

sity by recording both at various distances from a light source. Light intensity was measured using a digital photometer (Spectra model Professional IV A).

These trials were performed with the Rug Warrior robot, which was running the Vehicle 1.5 program. All conditions were the same except that the floor of the tank was covered with a large, flat and (most importantly) dry covering. Three additional trials were performed with the Rug Warrior, in which its initial orientation was 180 degrees different from that in the initial trials.

4 Results

4.1 The Aquatic Robot

Before the light source was turned on, the robots tail was biased very far to the right and the robot rotated in three small clockwise circles (Figure 7). This was the case for all three trials with the swimming robot. Moreover, these first three circles were small and were centered around roughly the same point. Once the light source was turned on, an immediate reaction was seen in the tail, which moved less biased to the side. After several tail beats, a change was also seen in the heading of the robot. Its trajectory began to straighten out, which carried it away from its initial position, up the light gradient, until it was at, or near, the point of maximum light intensity. Once this happened, the robot began to rotate, in the clockwise direction, around the light source. This rotation continued until the end of each trial, such that by the end of the trial the robot had completed three more clockwise circles that were centered, roughly, around the point of maximum light intensity.

In order to take the qualitative description of the trajectory and quantify the important aspects, the heading of the robot was calculated. The heading was understood to be, essentially, the instantaneous orientation of the robot. As before, an orientation of 0 occurred when the robot was pointing directly along the x-axis, in the positive direction. From the calculation of heading, the change of heading was also determined (Figure 8). In some ways this measure is more important to consider, since it quantifies how much the robot was rotating. The amount of rotation, as discussed before, has been shown to be the essential control variable in HK (Crenshaw, 1993a, 1993b). By inspecting the change in heading over the course of the trials, one can see how the rotation remains fairly constant, in the negative (clockwise) direction, until the light source is turned on, at which time it moves closer to 0, indicating a straighter heading as the robot moves up the light gradient. As the robot begins to rotate around the source, the change in heading becomes more negative again, and remains there until the end of the trial.

A strong correlation existed between the change in heading and the light intensity at the sensor (Figure 8). Linear regressions were performed on data from all three trials and were statistically significant ($p < .0001$) with all three coefficients of determination (r^2) greater than 0.75. An 11point central running average was performed on the change of heading data used in the statistical

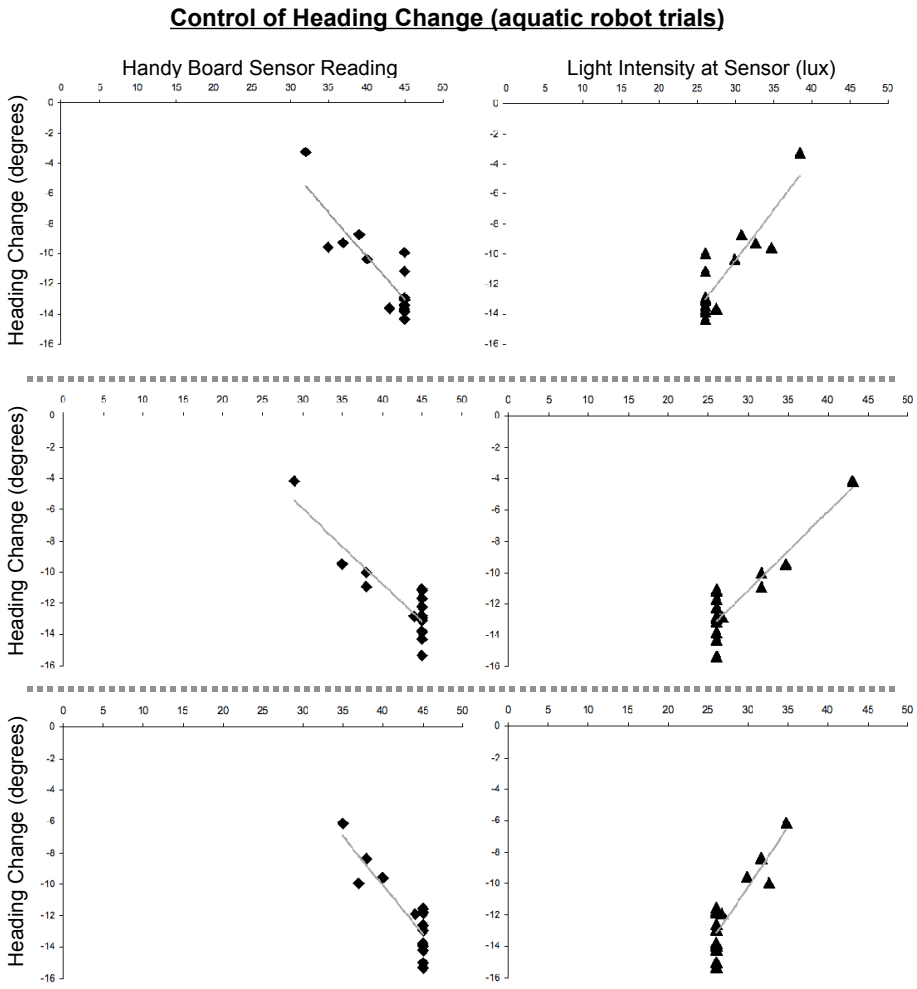

Figure 7: The aquatic robot controlled its rotational velocity, or heading change, in proportion to light intensity at the sensor. In these graphs, heading change is shown, as it relates to the sensor readings of the robot and to light intensity at the sensor. Data from the three trials are shown from top to bottom. The gray lines represent linear regressions, all of which were significant ($p < .05$).

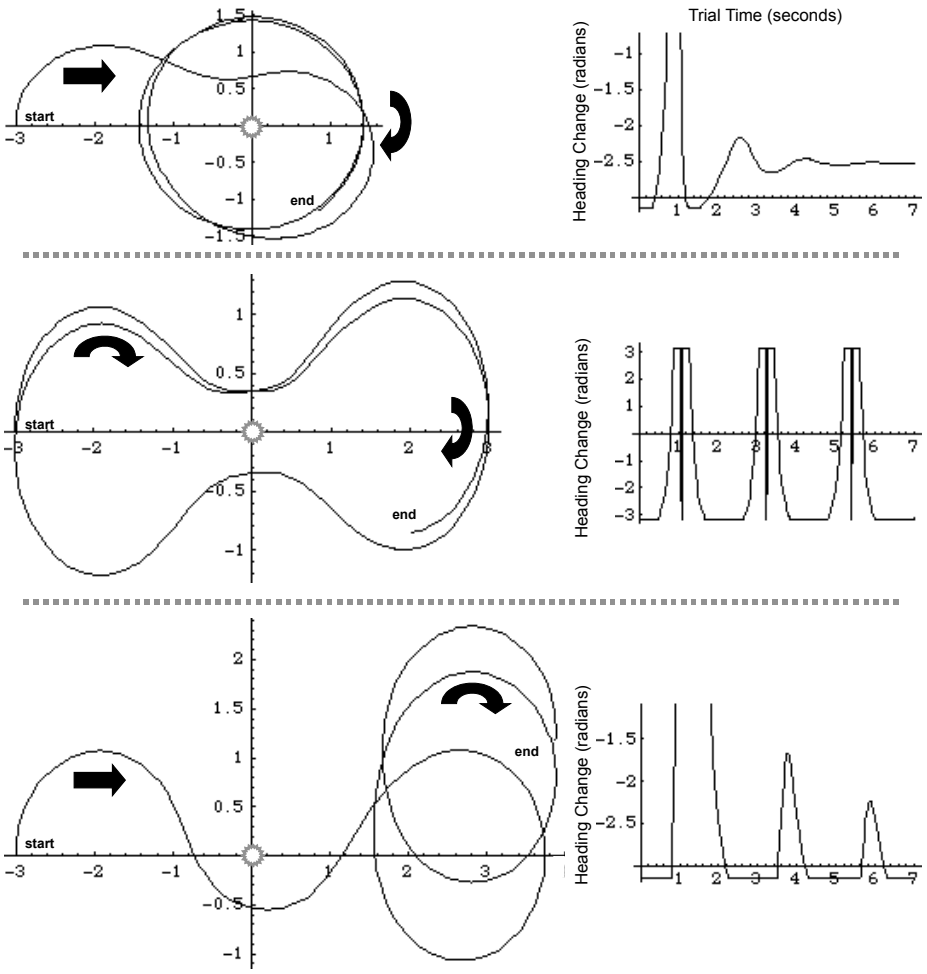

Figure 8: The simulated agent, as seen with three different sensor orientations. Shown from top to bottom, the sensor orientations were 45°, 90° and 180° from straight forward, respectively. Trajectory graphs are shown to the left, and to the right are the corresponding graphs showing heading change over time. The starting and ending positions are labelled, as is the point of maximum light intensity (sun symbol). The direction of rotation is also indicated with arrows.

analysis. This was done because the gathered data had substantial amounts of noise.

4.2 The Simulated Agent

The simulated agent, starting at a position away from the source, moves up the light gradient and towards the source (Figure 9). As it approached the source, it falls into a circling pattern which continues infinitely, in the unchanging conditions of the simulation. This is very similar to the results from the aquatic robot. However, at slightly further starting distance the agent takes a less direct route to fall into its final circling pattern. The agent will begin a rotation that is biased towards the source, causing the agent to drift in the direction of the source. When the drift brings the agent to a critical distance near the source, the agents path will then be more direct, and will bring it up the gradient to the source. At still further distances from the source, the light intensity will never be high enough to trigger a response from the agent. Thus, it will simply rotate in circles forever.

The ability of the agent to perform positive gradient orientation can be altered, and even reversed by adjusting one variable. That variable is the directionality of the sensor with respect to the body (Figure 9). When the sensor is placed from about 45° to -45° (with 0 being directly in front), the agent will orient positively to the light source and circle in the standard fashion, like the aquatic robot. With a sensor position more towards the sides of the agent, the orientation never achieves a circling behavior around the source. Instead, the agent tends to wander slightly away from the source before rotating and returning. If the sensor is placed towards the back of the agent, negative orientation is what occurs. Indeed, the agent will enter a biased rotation that moves steadily, if not directly, away from the light source.

4.3 Vehicle 1.5

All trials with the Vehicle 1.5 control scheme had a strong resemblance to those with the aquatic robot (Figures 10 and 11). The robot performed tight, clockwise circles in the dark. After the light source was turned on, the robot moved up the light gradient and finished the trials by performing clockwise circles around the light source. In the trials where the robot was initially placed in the same initial position as the aquatic robot, the act of moving up the light gradient also involved an apparent zeroing of the rotational velocity. That is, the robot moved nearly straight up the light gradient towards the light source. However, in the trials where the initial position was 180 degrees in the opposite direction, the robot did a pronounced counter-clockwise turn before straightening out and moving up the light gradient.

As with the aquatic robot, the heading and change of heading were calculated for each trial with Vehicle 1.5 (Figures 10 and 11). The results were very similar, as well. The change of heading over each trial remains fairly steady until the light is turned on, at which point there is a significant increase, as the robot moves

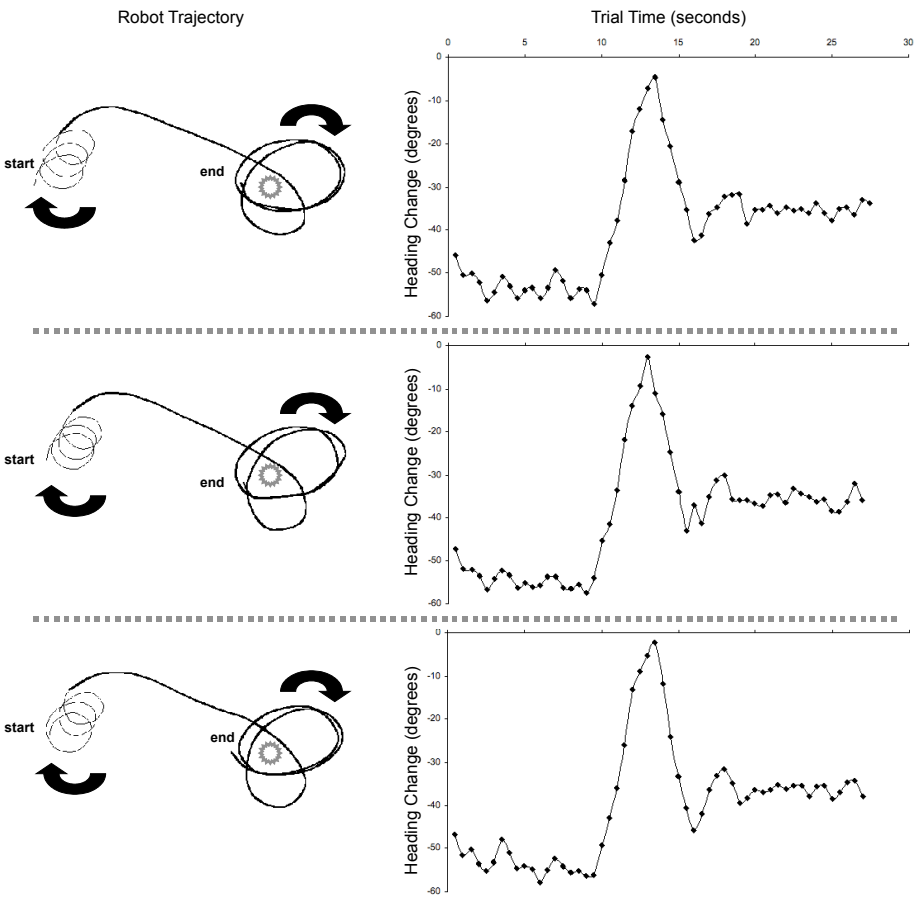

Figure 9: Vehicle 1.5 was put through three trials, shown from top to bottom, in which the initial orientation was 90° away from the light source. Trajectory graphs are shown to the left, and to the right are the corresponding graphs showing heading change over the course of the trials. The starting and ending positions are labelled, as is the point of maximum light intensity (sun symbol). The direction of rotation is also indicated with arrows. The heading change graphs display the data after an 5-point central running average was performed.

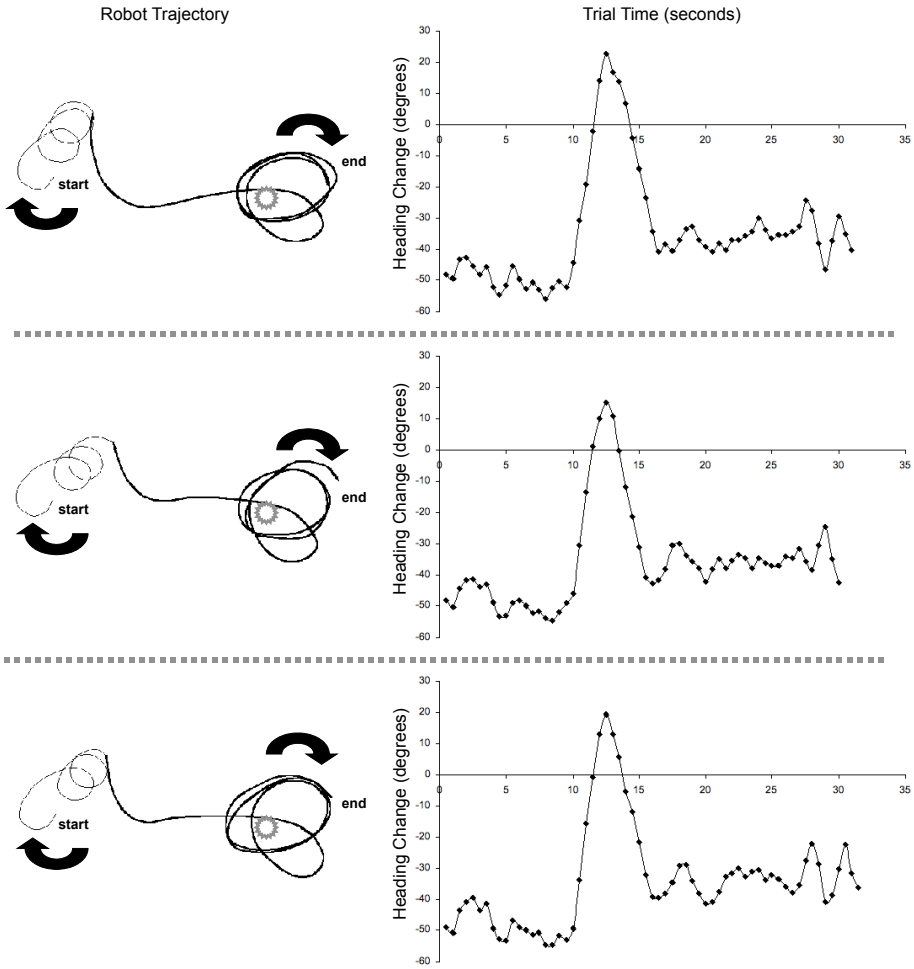

Figure 10: Vehicle 1.5 was put through three trials, shown from top to bottom, in which the initial orientation was 270° away from the light source. Trajectory graphs are shown to the left, and to the right are the corresponding graphs showing heading change over the course of the trials. The starting and ending positions are labelled, as is the point of maximum light intensity (sun symbol). The direction of rotation is also indicated with arrows. The heading change graphs display the data after an 5-point central running average was performed.

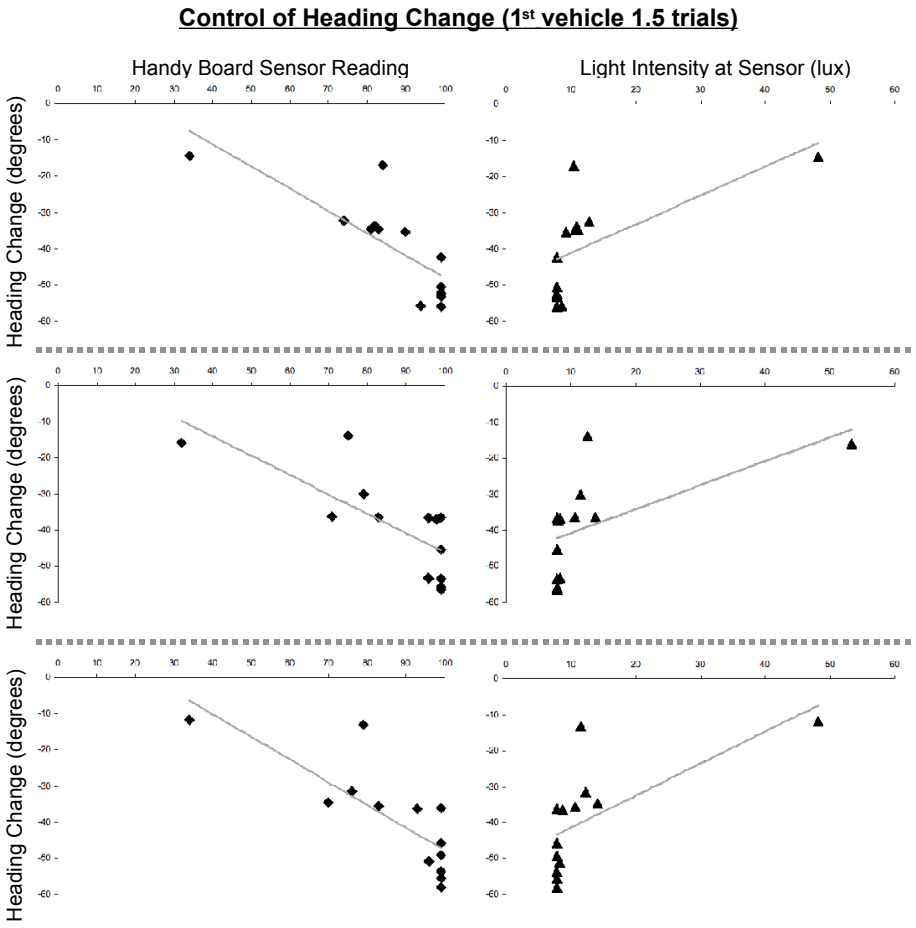

Figure 11: Vehicle 1.5 controlled its rotational velocity, or heading change, in proportion to light intensity at the sensor. In these graphs, heading change is shown, as it relates to the sensor readings of the robot and to light intensity at the sensor. Data from the three trials, with initial orientation at 90°, are shown from top to bottom. The gray lines represent linear regressions, all of which were significant ($p < .05$).

up the light gradient. In the trials where a counter-clockwise turn occurred, an impressive spike into the positive numbers can be seen. Finally, there is a settling back down of the numbers as the robot rotates around the light source for the remainder of the trial.

A strong correlation also existed between the change in heading and the light intensity at the sensor in these trials (Figure 12). Linear regressions were performed on data from all six trials and all were statistically significant. However, for the first three trials, where the initial position was the same as for the aquatic robot, the numbers were not quite as significant (all $p < .02$ and $r^2 > 0.34$) as with the second set of three (where $p < .0001$ for all, and all $r^2 > 0.7$). A 5point central running average was performed on the change of heading data used in the statistical analysis. This was done because the gathered data had substantial amounts of noise.

5 Discussion

Using a single sensory input and only one degree of freedom in motor output, the aquatic robot managed to properly orient to a light source, move up the gradient from a position of lower light intensity and hold station near the point of maximum intensity. The simulated agent was also able to perform the same behavior. Moreover, with a single sensory input, and two simple motor connections (one excitatory and one inhibitory), Vehicle 1.5 was able to properly orient to a light source and hold station near the light source. All three of these systems utilized 2D cHK, even if the control mechanisms look slightly distinct. They each performed phototaxis by modulating their rotational velocity. In all cases, rotational velocity was modulated through simple linear control mechanisms, with respect to the intensity of light.

5.1 The Aquatic Robot

The trajectories of the aquatic robot described here, were quite different in some ways from the aquatic robot used by Long et al. (2003a). Fortunately, they seemed to be different in all the ways that it was predicted they would be different. That is, it seems that the attempt to make improvements on the experiments of Long et al. (2003a) was a success. Primarily, the experiments described here have a complete absence of effects from the wall of the tank. Thus, one can see from our experiments how the aquatic robot performs without the help or hindrance of the tank walls. Obviously, the fact that the robot still properly orients to the light source without these effects makes a strong positive statement about this control scheme. The walls do not provide a necessary aid for the aquatic robot to perform gradient orientation. Indeed, it seems reasonable to conclude that it could perform cHK in an environment with no walls whatsoever. The aquatic robot carries out 2D cHK on its own.

Another interesting aspect to notice about the aquatic robot described here, is that its trajectories more accurately reproduce the trajectory predicted by the

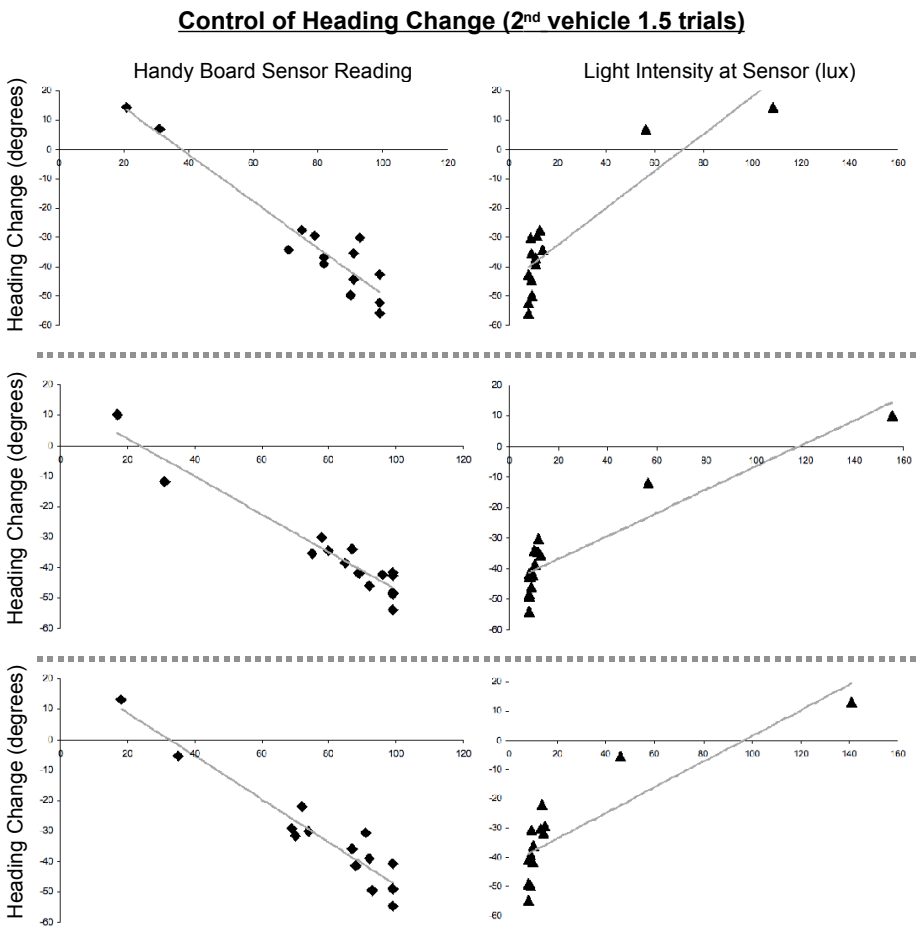

Figure 12: Vehicle 1.5 controlled its rotational velocity, or heading change, in proportion to light intensity at the sensor. In these graphs, heading change is shown, as it relates to the sensor readings of the robot and to light intensity at the sensor. Data from the three trials, with initial orientation at 270°, are shown from top to bottom. The gray lines represent linear regressions, all of which were significant ($p < .05$).

analytic solution to 2D HK, as discussed by Long et al. (2003b) and the dynamic simulation described in this paper. Both of these models show how the agent holds station near the light source by circling it clockwise. Notably, the trajectories of the Long et al. (2003a) aquatic robot, while still exhibiting phototactic behavior, did not show the characteristic clockwise circling. Instead, that robot appeared to hold station by performing relatively small, counter-clockwise circles around and through the light source. The aquatic robot described here does exhibit the clockwise station holding. Since this matches the behavior predicted by the analytic solution, and since the behavior seen in the first aquatic robot has not been seen in any other 2D HK system, the behavior of the aquatic robot described here is viewed as an improvement. This improvement has resulted from the elimination of wall effects, the tightening of sensorimotor connections and the overall improvement of swimming ability.

5.2 The Simulated Agent

The simulated agent utilizes information about the forces involved in the aquatic system to show how phototactic behavior arises. The tail of the aquatic robot produces a thrust that gives the robot a translational velocity. However, any asymmetry in the position of the tail with respect to the body leads to a decrease in translational velocity, and the creation of a rotational velocity. This rotational velocity is, of course, the control variable for producing phototaxis. This look at the dynamics of the aquatic robot is simple, and many assumptions are made to keep it simple. In the simulation, thrust is constant, drag is simply stated and a steady state is assumed. However, even in this system with simplified dynamics, the behavior of the agent definitely displays phototaxis.

Furthermore, the motion of the agent is nearly indistinguishable from the kinematic analysis offered by Long et al. (2003b). The only appreciable difference is that the agent never reaches a point where its orbits around the gradient source are exactly symmetrical. There is always some oscillation in heading change, though that oscillation may become very small (amplitude less than .001°). A similar, but more substantial, oscillation can also be seen in the aquatic robot (amplitude remaining as high as 2°). However, in the analytic solution to 2D cHK, the point of no oscillation is reached at the exact moment that the agent reaches its critical proximity to the source. The dynamical model, thus, falls somewhere between the analytic solution and the actual system. This makes sense given that it falls between them in terms of how many variables it includes. The kinematic model is highly idealized with respect to the dynamical model and the physical system has many variables for which the dynamical model doesnt account.

This simulated agent also functions as a source of independent evidence for several claims made by Long et al. (2003b), concerning their analytic solution to 2D HK. First, it reinforces how sensor placement can alter the resultant behavior of an agent performing 2D HK. Standard sensor placement, with forward-facing orientation, results in positive phototaxis, whereas back-facing sensor placement results in the opposite. With a sensor placed to the side of the agent, a

wandering behavior arises. These findings still have yet to be experimentally supported. Another important claim which this model supports is that 2D HK is possible within any vector field, and with any directional sensor meant to function within that field. Using light gradients for the robotic experiments in this paper was merely a matter of convenience. Light gradients are easy to produce and maintain. However, the robust 2D HK control scheme could function within any number of vector fields, given the appropriate sensor. Long et al. (2003b) noted that vector fields in which 2D HK could take place are as diverse as light, gravitational, magnetic and electric field.

5.3 Vehicle 1.5

The vehicles developed by Valentino Braitenberg (1984) were thought experiments. More than that, they were experiments in synthetic psychology, whereby the basics of neuroanatomy could be applied in amazingly simple ways to create agents with complex behaviors. The creation of Vehicle 1.5 was also a thought experiment, but of the opposite type. Instead of synthetically combining parts to see the end product, this thought experiment looked at a whole behavior and attempted to break it down into its most basic manifestation. Thus, the goal of the experiment was to get down to basics, while still maintaining the whole of the behavior. If getting down to basics resulted in no longer having a phototactic system then the experiment would have been a failure.

More specifically, though, the experiment had to produce a very specific kind of phototaxis, 2D HK. The implementation of the Vehicle 1.5 control mechanism is so different from other 2D HK control mechanisms. Hence, it is not obvious that Vehicle 1.5, even if it produced phototaxis, would produce phototaxis via 2D HK. Getting down to basic mechanisms to produce phototaxis, but eliminate 2D HK would have also been a failure. At the very least, it would have become a topic for a different discussion, not a discussion about 2D HK.

Hence, we are left with two very important questions to ask about Vehicle 1.5, the product of our thought experiments. The first question is whether Vehicle 1.5 can perform phototaxis. Secondly, can it perform phototaxis by way of 2D HK? These can be answered by looking to the experimental results. Fortunately, both questions can be answered affirmatively, as well. Phototaxis can clearly be seen by looking at the trajectories of the robot. The robot orients to the light gradient very effectively. Moreover, it appears that the trajectories bear great resemblance to the other systems, said to perform 2D HK. The robot, in all instances, circles clockwise in the dark and, in the presence of light, straightens its path to carry itself up the light gradient. Moreover, it always ends its run by circling the light source clockwise. Likewise, this type of trajectory is shared by the aquatic robot, the analytic model of Long et al. (2003b), and the simulated agent described here. Perhaps more convincing than appearances, though, is that Vehicle 1.5 varies its rotational velocity in proportion to light intensity like the aquatic robot does.

Vehicle 1.5, then, is an agent that performs phototactic behavior by utilizing 2D HK. Moreover, this vehicle uses only two simple linear connections, like those

described by Braitenberg (1984) to link sensory information and motor output. Also, it controls only two motors with those sensorimotor connections. Vehicle 1.5 has these two motors and two connections in common with Braitenbergs simplest tactic vehicle, Vehicle 2. However, since it only utilizes one sensor, it constitutes a perception-action loop that is simpler than Vehicle 2, which uses 2 sensors, and implies that Vehicle 2 has some amount of redundancy in the way it navigates. It is clear from Vehicle 1.5, that only one sensor is necessary for this type of navigation.

6 Conclusions

This system, 2D HK, may not be the most effective system for navigating with respect to vector fields in 2D actuation space. Trajectories are characteristically curvilinear, and consequently longer than more complex systems of navigation. However, 2D HK may be the simplest system for performing this type of navigation. Only a single, directional sensory input is needed to effectively carry out 2D HK. Moreover, it is only necessary to modulate a single control variable, the rotational velocity, which can be done by utilizing as few as one actuator. The sensorimotor connections, too, can be simple, linear functions linking sensation and motor output.

The 2D HK system is also robust, capable of operating in a real-world environment and well as an idealized computer simulation. It can function by making use of any vector-based sensor, and within any number of vector fields. Furthermore, different implementations of the control scheme will work, even with drastically different actuation styles. As long as the perception-action loop is preserved (i.e. rotational velocity modulated in proportion to stimulus intensity) 2D HK will allow navigation within a gradient.

References

R.C. Arkin. *Behavior-Based Robotics*. MIT Press, 1998.

V. Braitenberg. *Vehicles: Experiments in Synthetic Psychology*. MIT Press, 1984.

R.A. Brooks. *Flesh and Machines: How Robots Will Change Us*. Pantheon Books, 2002.

H.J. Chiel and R.D. Beer. The brain has a body: adaptive behavior emerges from interactions of nervous system, body and environment. *Trends Neurosci.*, 20:553–557, 1997.

H.C. Crenshaw. Orientation by helical motion. i. kinematics of the helical motion of microorganisms with up to six degrees of freedom. *Bull. Math. Biol.*, 55: 197–212, 1993a.

H.C. Crenshaw. Orientation by helical motion. iii. microorganisms can orient to stimuli by changing the direction of their rotational velocity. *Bull. Math. Biol.*, 55:231–255, 1993b.

H.C. Crenshaw. A new look at locomotion in microorganisms: rotating and translating. *Amer. Zool.*, 36:608–618, 1996.

G. Fraenkel and D.L. Gunn. *The Orientation of Animals: Kinesis.* Oxford, 1940.

D. Halliday, R. Resnick, and J. Walker. *Fundamentals of Physics.* John Wiley & Sons, Inc., 2001.

D. Kelley. *The Evidence of the Senses: A Realist Theory of Perception.* Louisiana State University Press, 1986.

M. Kemp. Micro-auvs ii: Control. In *12th UUST*, 2001.

M. Kemp, H. Crenshaw, B. Hobson, J. Janet, R. Moody, C. Pell, H. Pinnix, and B. Schulz. Micro-auvs i: platform design and multi-agent system development. In *12th UUST*, 2001.

A.C. Lammert and J.H. Long. Biorobotics: Can robots mimic the phototactic behavior of sea squirt larvae? Vassar College URSI Symposium, 2003.

J.H. Jr. Long, A.C. Lammert, J. Strother, and M.J. McHenry. Biologically-inspired control of perception-action systems: Helical klinotaxis in 2d robots. In *13th UUST*, 2003.

J.H. Jr. Long, A.C. Lammert, C.A. Pell, M. Kemp, J. Strother, H.C. Crenshaw, and M.J. McHenry. A navigational primitive: Biorobotic implementation of cycloptic helical klinotaxis in planar motion. *Oceanic Engineering*, in review.

M.J. McHenry and J. Strother. The kinematics of phototaxis in larvae of the ascidian aplidium constellatum. *Mar. Biol.*, 142:173–184, 2003.

T.M. Morse, T.C. Ferree, and S.R. Lockery. Robust spatial navigation in a robot inspired by chemotaxis in caenorhabditis elegans. *Adaptive Behavior*, 6:393–410, 1998.

R.R. Murphy. *Introduction to AI Robotics.* MIT Press, 2000.

R. Pfeifer and C. Scheier. *Understanding Intelligence.* MIT Press, 1999.

E.M. Purcell. Life at low reynolds number. *Am. J. Physics*, 45:3–11, 1977.

S. Russell and P. Norvig. *Artificial Intelligence: A Modern Approach.* Prentice Hall, 2003.

B. Webb. Robots in invertebrate neuroscience. *Nature*, 417:359–363, 2002.

C.M. Young. *Behavior and locomotion during the dispersal phase of larvae life.* CRC Press, 1995.